Available online at www.sciencedirect.com

ScienceDirect

Energy Procedia 69 (2015) 1068 – 1077

Energy Procedia

International Conference on Concentrating Solar Power and Chemical Energy Systems, SolarPACES 2014

Single-tank TES system – Transient evaluation of thermal stratification according to the second-law of thermodynamics

Simone A. Zavattoni[a], Maurizio C. Barbato[a,*], Andrea Pedretti[b], Giw Zanganeh[b]

[a]*Department of Innovative Technologies, SUPSI, 6928 Manno, Switzerland,*
[b]*Airlight Energy Manufacturing SA, 6710 Biasca, Switzerland.*

Abstract

Single-tank thermal energy storage (TES) systems represent a valuable alternative, to the most common two-tank systems with molten slat, to effectively store thermal energy in concentrating solar power (CSP) applications. From an economic standpoint, the gap between the two TES solutions is relevant. A remarkable cost reduction can be achieved if a single-tank TES system, with a low-cost filler material, is exploited. In this kind of TES system, the buoyancy driven effects of the heat transfer fluid are exploited to establish and maintain a thermocline zone which separates the hot region on top and the cold region at the bottom of the tank. The thinner the thermocline thickness, the higher the thermodynamic quality of the stored energy.
As soon as the TES is charged for the first time, i.e. startup of the system, the extent of thermal stratification may vary sharply during the first cycles before achieving a stable condition. For this reason, this study aims at evaluating, by means of accurate time-dependent 3D CFD simulations, the transient evolution of thermal stratification of a single-tank TES system exploited to fulfill the round-the-clock energy requirement of a reference 80 MW_e CSP plant which uses air as heat transfer fluid. A total of 30 consecutive cycles, composed by charge/discharge phases, were simulated. Since the thermal energy stored is exploited to produce electrical energy, the performances of the TES system, operating under cyclic conditions, were qualitatively characterized by means of a stratification efficiency index based upon the second-law of thermodynamics.

Peer review by the scientific conference committee of SolarPACES 2014 under responsibility of PSE AG

Keywords: thermal stratification; packed bed; thermal energy storage (TES); second-law efficiency; effective thermal conductivity (ETC); computational fluid dynamics (CFD); entropy generation; exergy; concentrating solar power (CSP).

* Corresponding author. Tel.: +41 058 666 6639.
E-mail address: maurizio.barbato@supsi.ch

Peer review by the scientific conference committee of SolarPACES 2014 under responsibility of PSE AG
doi:10.1016/j.egypro.2015.03.213

1. Introduction

In the field of concentrating solar power (CSP) technology, the topic of thermal energy storage (TES) showed a remarkable increase in terms of research and development efforts by industries, national laboratories and universities. Thermal energy can be stored in the form of sensible or latent heat; on the basis of the TES systems in operation it is evident that sensible heat is by far the most implemented solution. The two-tank system with molten salt, either direct or indirect, is generally exploited in conventional CSP plants. A remarkable TES cost reduction can be achieved by replacing the latter with a single-tank system with low-cost filler material [1]. This solution may found a large applicability in the case the CSP plant uses air as heat transfer fluid (HTF), as for the novel CSP solution developed by the Swiss company Airlight Energy Manufacturing SA [2]. Their innovative technology involves the use of a reliable TES system based on a packed bed of gravel. Being a single-tank solution, the buoyancy-driven effects of the HTF are exploited to establish and maintain a thermocline zone which separates the hot region on top and the cold region at the bottom of the tank. The thinner the thermocline, the higher the thermodynamic quality of the stored energy, i.e. higher exergy content. However, the extent of thermal stratification may vary sharply during cycles especially during the startup when the TES is charged for the first time. In this case, computational fluid dynamics (CFD) simulations are a useful tool which allows, during the design phase, to analyze the thermo-fluid dynamics behavior of the TES system focusing on the optimization of its thermal stratification capability.

2. Qualitative evaluation of thermal stratification based on the second-law

Defining a proper index for characterizing, and comparing, thermal stratification in TES processes has been the subject of several studies [3-6]. On the basis of the accuracy and complexity of the methods developed, three main categories may be identified: (i) dimensionless numbers, e.g. Reynolds, Richardson, Grashof, Peclet, Biot and Fourier numbers [5]; (ii) efficiency indexes based upon the first law of thermodynamics, i.e. energy balance of the system under consideration; (iii) efficiency indexes based upon the second law of thermodynamics or miscellaneous, i.e. combination of the two laws. Since, in the case of CSP, the thermal energy stored is then used to produce electrical energy, a system characterization based upon methods belonging to category (i) or (ii) has only a limited usefulness because none information about the thermodynamics quality of the stored energy can be obtained. In fact, considering two ideal TES systems, one perfectly stratified and the other fully-mixed, despite having the same amount of stored energy, the exergy content may be substantially different. For this reason, second-law based methods, introducing the concept of entropy generation and exergy, shall be preferred among others. Exergy is a measure of the work potential of a given amount of energy or, in other words, the maximum amount of energy that can be extracted from the system, at the specified state, as useful work. Since the work output is maximized, a fully-reversible process is assumed to occur between the specified, or actual, state of the system and its dead-state, i.e. thermodynamic equilibrium with its environment [7]. Therefore, the amount of incoming energy into the TES cannot be entirely recovered and consecutively converted into useful work because there will always be a certain amount of unavailable energy, i.e. difference between the total energy of a system at a specified state and the exergy of that energy.

Thanks to the advantage of being directly applicable in conjunction with a CFD-based analysis, the stratification efficiency, given by the so-called entropy generation ratio [5], was exploited to evaluate the transient evolution of thermal stratification into the industrial-scale TES unit. The qualitative information obtainable, by using this second-law based approach, is the extent to which the real TES system under investigation approaches the ideal case of perfectly stratified TES. Therefore, for any instant of time, the energy and entropy change of the system, with respect to the initial dead-state, was computed. The thermal energy stored into the real TES, at the time considered, was then arranged to obtain the two idealized cases of perfectly stratified and fully-mixed TESs. In the case of perfectly stratified TES, the packed bed was divided into two adiabatically-separated regions, the one at high temperature on top and that at low temperature at the bottom, corresponding to the highest and the lowest temperatures observed into the real TES. Instead, the idealized fully-mixed TES was obtained by assuming the entire packed bed at an average temperature. The entropy change was then computed for the two ideal cases also

with respect to the same initial dead-state of the real TES. Therefore, the entropy change of the real TES must always be included between that of the ideally stratified and the fully-mixed cases respectively, thus:

$$\Delta S_{fully-mixed} \geq \Delta S_{real} \geq \Delta S_{stratified} \tag{1}$$

The stratification efficiency, corresponding to the quality of the stored energy, may be defined as:

$$\eta_{REG} = \frac{\Delta S_{fully-mixed} - \Delta S_{real}}{\Delta S_{fully-mixed} - \Delta S_{stratified}} \tag{2}$$

Stratification efficiency close to unity indicates that the real TES is operating with a sharp thermal stratification, i.e. the entropy generation is minimized, and the thermal energy is stored at the highest thermodynamic quality.

3. Industrial-scale TES system

The single-tank TES system was dimensioned in order to fulfill the round-the-clock energy requirement of a reference 80 MW_e CSP plant based upon the Airlight Energy technology [2][8]. Considering the foreseen advantages in terms of availability, affordability and reliability, a packed bed of natural rocks, 3-4 cm average particle diameter, was exploited as low-cost filler material. The latter is contained into a well-insulated concrete vessel with a truncated-cone shape in order to minimize the effect of thermal ratcheting on the lateral walls. It is also buried into the ground avoiding the need of a strong containing structure.

Thanks to the highest monthly DNI, the month of June was selected as reference for dimensioning the TES system. Air is the HTF for the entire CSP plant. The HTF temperature, coming from the solar field, and fed through the storage, is 650 °C; whereas, after the power block heat exchangers (HEs), the HTF temperature is reduced down to 270 °C. During the charge phase, the HTF at high temperature flows downward through the packed bed delivering its thermal energy to the gravel. Instead, during the discharge phase, the energy stored can be recovered by reversing the air-flow direction with the HTF coming from the heat exchangers of the power block. Hence, 650 °C and 270 °C were assumed as reference charging and discharging temperatures respectively. Calculations showed that a total of 7 TES units, 25.7 m and 21.7 m the upper and the lower diameter respectively and 9.5 m packed bed height, are required to hold the whole volume of about 30,000 m^3 of rocks [9]. The thermal capacity of each TES unit, defined as the total energy stored in the bed when charged from ambient temperature to isothermal conditions at the inlet air flow temperature of 650 °C, is 1 GWh_{th}.

With the aim of obtaining a proper velocity distribution of HTF through the packed bed, as similar as possible to a plug flow, it was decided to equip each of the TES unit with four pipes on top, and four pipes at the bottom respectively, rather than a single pipe located in the center. Furthermore, two calm chambers, 1 m high, were also designed on top and at the bottom of the packed bed.

4. CFD modeling

Left-hand side of Fig. 1 shows the CAD model of one of the seven units. The TES system is symmetric leading hence to the possibility of considering only a quarter of the whole unit as computational domain. It was discretized with a grid of almost 1,150,000 hexahedral elements. Right-hand side of Fig. 1 shows the main boundary conditions applied to the model.

Navier-Stokes, energy, turbulent kinetic energy and turbulent dissipation rate transport equations were numerically solved with the finite volume method (FVM) approach [10] by means of Fluent 14.5 code from ANSYS. The realizable k - ε model [11], with standard wall functions [12], was selected to account for turbulence effects; full-buoyancy effects on the turbulent kinetic energy, and on its dissipation rate, were also considered [13].

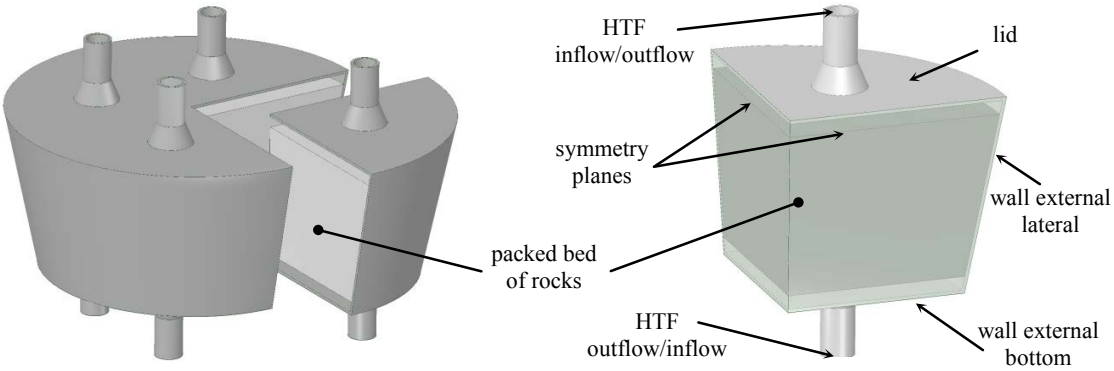

Fig. 1. Schematic CAD model of a single TES unit (l.h.s.) and main boundary conditions applied to the computational domain considered (r.h.s.).

Thermal energy losses by means of conduction through the ground and convection/radiation from the lid towards the environment were accounted for. The environment temperature was assumed equal to 308.15 K and 293.15 K during charging and discharging respectively. The layers of concrete and insulating materials were numerically modeled, by means of the shell-conduction approach [14], with a material of equivalent thermo-physical properties.

In order to evaluate the effect of startup operation on thermal stratification, at the beginning of the time-dependent CFD simulation, namely at time t = 0 sec, the TES system unit was considered in thermal equilibrium with the environment with a dead-state temperature of 290.15 K.

The rock-bed was treated as a continuum since both the criterions given by the dimensionless bed size $L/d_p >> 10$, i.e. the minimum bed dimension L over the particle diameter d_p, and the size parameter $\xi = \pi \cdot d_p/\lambda >> 5$, i.e. the particle size relative to the important wavelengths λ of the radiation, are verified [15]. Therefore, the packed bed was modeled exploiting the porous media approach [16]. With this strategy, the porous medium is characterized by means of four main parameters namely: the effective thermal conductivity (ETC), the void-fraction distribution, the permeability K and inertial resistance coefficient C_2 (related to the pressure drop evaluation). Besides the dimensionless bed size and since the variation of temperature across d_p is negligible compared to that across L [17], local thermal equilibrium (LTE model) between the solid matrix and the fluid phase was assumed; therefore, a single conservation equation of energy is solved to model the heat transfer through the porous medium.

4.1. Evaluation of stratification efficiency

The transient stratification efficiency of the TES system was evaluated according to the methodology detailed in section 2. A user-defined function (UDF), i.e. a “C” routine properly written to be linked to the CFD solver, was implemented into Fluent and assigned to the porous medium, with the aim of gathering the main results of the CFD simulation which are required to evaluate the stratification efficiency.

Once executed, the UDF allows to perform a loop over all the computational cells of the porous medium in order to collect information such as temperature, volume and absolute position of each cell.

Based upon an arbitrary number of divisions, the packed bed is virtually divided, in the axial direction, into a multilayer zone of constant thickness. According to a preliminary sensitivity analysis, a total of 75 layers were assumed as reference number of divisions of the packed bed. Therefore, with 9.5 m as the packed bed height, the resulting thickness of each layer is about 0.127 m. All the cells information are automatically stored into the proper layer according to the axial position of each cell. The temperature of each layer is then computed by means of a volume-averaging technique. The resulting array, containing the temperature and the volume of each layer, is automatically exported and post-processed. The gathered values were exploited to compute the total amount of energy and exergy available into the packed bed along with the entropy change of the TES during the process. On the basis of the total amount of available energy, the two ideal conditions of perfectly stratified and fully mixed TES were derived. The entropy change was also computed for the two ideal conditions obtaining the required threshold values for computing the thermal stratification based upon the second law of thermodynamics.

4.2. Effective thermal conductivity and heat transfer in packed beds

Over the last decades, the topic of heat transfer in packed beds, and especially the determination of the effective stagnant thermal conductivity (ETC), has been the subjects of several theoretical, experimental and numerical investigations [15]. The simplest models developed, to compute stagnant ETC, assume that the solid and the fluid phases can be considered as different layers positioned either in parallel or in series with respect to the direction of the heat flow. More sophisticated approaches are based on a detailed description of the physics behind heat transfer in packed beds. According to the theoretical and experimental studies of Yagi and Kunii [18], earlier, and Kunii and Smith, afterwards [19], the heat transfer mechanisms in packed beds of unconsolidated particles can be considered as the sum of two contributions: the heat transfer mechanisms independent on the fluid flow and those dependent on the lateral mixing of the fluid. In the case of packed bed with stagnant fluid, five different heat transfer mechanisms take place: (1) thermal conduction through solid, thermal conduction (2) through the contact surfaces of two packings and (3) through the fluid film near the contact surface of two packings, radiant heat transfer (4) between surfaces of two packings and (5) between neighboring voids. The latter two have to be intended in the case the fluid is a gas. The remaining heat transfer mechanisms, occurring when fluid flows through the packed bed, are: (6) heat transfer by convection solid-fluid-solid and (7) heat transfer by advective mixing. On the basis of heat transfer mechanisms (1) to (5), the authors derived a model for predicting the stagnant ETC of the packed bed, made by homogeneous spheres, that reads [19]:

$$k_{ETC}^{0} = k_g \cdot \left[\varepsilon \cdot \left(1 + \frac{\beta \cdot h_{rv} \cdot d_p}{k_g} \right) + \frac{\beta \cdot (1-\varepsilon)}{\left(\frac{1}{\varphi} + \frac{d_p \cdot h_{rs}}{k_g} \right)^{-1} + \frac{2}{3} \cdot k} \right] \tag{3}$$

wherein k_g is the HTF thermal conductivity; ε is the void-fraction of the packed bed; k is the fluid-to-solid thermal conductivity ratio. The geometric factor β is related to the particles arrangement: in the case of close packing of spheres it assumes the value of 0.895; conversely, for the most loose packing its value should be unity. Therefore, for almost all actual packed beds, β ranges between 0.9 and 1.

The radiation heat transfer coefficients h_{rv} and h_{rs}, for the void-to-void and the solid surface to solid surface exchange respectively, are defined as follows [18]:

$$h_{rv} = 0.227 \cdot \left(1 + \frac{\varepsilon \cdot (1-\psi)}{2 \cdot \psi \cdot (1-\varepsilon)} \right)^{-1} \cdot \left(\frac{T}{100} \right)^3 \tag{4}$$

$$h_{rs} = \frac{0.227 \cdot \psi}{2-\psi} \cdot \left(\frac{T}{100} \right)^3 \tag{5}$$

in which ψ and T are the superficial emissivity, and the absolute temperature respectively, of the solid particles. The φ parameter represents the measure of the effective thickness of the fluid film adjacent to the contact surface of two solid particles. To overcome the complexity in the computation of the latter, Kunii and Smith proposed a simplification based upon the assumption that actually, all the packed beds may be considered as a combination of two basic packing states: the loose ($\varphi_1 : n_1 = 1.5$ with $\varepsilon_1 = 0.476$) and the close state ($\varphi_2 : n_2 = 4\sqrt{3}$ with $\varepsilon_2 = 0.26$) wherein n indicates the equivalent number of contact points. Hence, for a bed with a given void fraction, φ can be expressed as:

$$\varphi = \varphi_2 + (\varphi_1 - \varphi_2) \cdot \frac{\varepsilon - 0.26}{0.216} \quad \text{for} \quad 0.26 \le \varepsilon \le 0.476 \tag{6}$$

In the field of numerical modeling, stagnant ETC is commonly exploited to model heat transfer in porous media since it allows to group all the non-convective heat transfer mechanisms within a single equivalent value. The remaining heat transfer mechanisms (6) and (7), dependent on the fluid flow, are automatically accounted for by the numerical solution of the Navier-Stokes and energy transport equations.

Thanks to the satisfactorily CFD model validation with experimental data [20], the model derived by Kunii and Smith [19] was implemented, by means of purpose-built UDFs, into the CFD code to accurately describe the heat transfer into the industrial-scale packed bed TES system under investigation. Thermal radiation heat transfer was accounted for by the ETC itself and hence none additional radiation model was activated for the computation.

4.3. Void-fraction distribution in a generic packed bed of spherical particles

The void-fraction of a generic homogeneous packed bed, defined as the ratio of the void volume with respect to the total bed volume, depends mainly on particles arrangement. In the case of randomly packed spherical particles, the reference porosity in the bulk region ranges between 0.36 - 0.43 [21].

Near the containing walls the arrangement of the particles is modified affecting the overall packing structure for a distance of about 5 particle diameters from the wall. In this near-wall region, the porosity distribution undergoes a sharp oscillatory variation, from a value close to unity to a minimum of 0.2 at a distance of 0.5 d_p, due to the presence of the containing walls [22]. Beyond the distance of about 5 d_p from the wall, the porosity approaches the value of the bulk region. Therefore, for real packed beds, there are two main conditions that entail to a porosity variation: (i) the wall effect or channeling (i.e. a porosity variation in the radial direction of the packed bed) and (ii) the thickness, or top-bottom, effect (i.e. a porosity variation dependent on the height of the packed bed).

The latter is considered negligible for almost all the practical cases; however, in the case of large-scale systems, the void-fraction variation in the axial direction of the packed bed can be relevant. Numerical CFD simulations, along with experimental data, allowed to observe a second-order monotonic decrease of the void-fraction with the packed bed depth [23][24]. Because of that, a quadratic void fraction distribution was implemented, into the CFD solver, in order to replicate the thickness effect. Instead, the effect of channeling was considered negligible since the characteristic ratio D_{vessel}/d_p is well above the suggested threshold value of 20 - 25 [25].

4.4. Permeability and inertial resistance coefficient

The permeability and the inertial resistance coefficient need to be specified when flows through porous media are modeled. The normal approach of CFD codes is to model the porous media by the addition, to the standard fluid flow equations, of a momentum source term which, for the simplest case of homogeneous porous media reads:

$$S_i = -\frac{\mu}{K} \cdot v_i - C_2 \cdot \frac{1}{2} \cdot \rho \cdot |v| \cdot v_i \tag{7}$$

where S_i is the source term for the *i-th* momentum equation, $|v|$ is the magnitude of the velocity. This momentum sink contributes to the pressure gradient in the porous cell, creating a pressure drop that is proportional to the fluid velocity (or velocity squared) in the cell [14]. The source term is composed of two parts: a viscous loss term, also known as "Darcy term" (the first term on the r.h.s. of eq. 7) and an inertial loss term (the second term on the r.h.s. of eq. 7). As long as the flow velocity remains sufficiently small, i.e. when the local Reynolds number Re_K is smaller than 100 [16], the flow regime may be considered as laminar and the second term on the r.h.s. of eq. 7 may be dropped resulting into a special form of the Darcy's law known as the Blake-Kozeny equation [16]. In the case of packed beds with homogeneous spherical particles, permeability and inertial resistance coefficient can be computed comparing the momentum source term (eq. 7), with the semi-empirical Ergun's equation [26].

$$\frac{|\Delta P|}{L} = \frac{150 \cdot (1-\varepsilon)^2}{d_p^2 \cdot \varepsilon^3} \cdot \mu \cdot v + \frac{1.75 \cdot (1-\varepsilon)}{d_p \cdot \varepsilon^3} \cdot \rho \cdot v^2 \tag{8}$$

where v is the flow velocity, P the pressure, μ and ρ the fluid dynamic viscosity and density respectively and ε is the void-fraction. Therefore, the two coefficients can be computed as follows:

$$K = \frac{d_p^2 \cdot \varepsilon^3}{150 \cdot (1-\varepsilon)^2} \tag{9}$$

$$C_2 = \frac{3.5 \cdot (1-\varepsilon)}{d_p \cdot \varepsilon^3} \tag{10}$$

Due to their dependency on the void fraction distribution, an additional UDF was designed and compiled into the CFD code in order to automatically compute the values of the two coefficients at each computational node based upon their axial position into the packed bed.

4.5. Physical properties of the materials involved and numerical details

The fluid phase was described as ideal gas with thermo-physical properties (specific heat, thermal conductivity and viscosity), as a function of temperature, assigned as piecewise linear interpolations of tabulated data available in the literature [27]. The thermo-physical properties of the solid materials (rocks and concretes) were experimentally measured, and extrapolated afterwards to cover a wider temperature range, by using Thikhomirov's and Kelly's correlations for thermal conductivity and heat capacity respectively [28][29]. The extrapolated values were then assigned to the corresponding material as piecewise linear profiles. The rocks superficial emissivity was evaluated on the basis of the experimental data gathered from a 6.5 MWh_{th} TES prototype [20].

The numerical solution of the governing equations was performed with the "pressure based" approach, which assumes that mass density depends on temperature and on a fixed pressure reference value [13]. Because of the relatively low velocity of the HTF throughout the TES system, and since none large pressure variations are expected into the computational domain, compressibility effects on the HTF flow were not accounted for.

All the model equations were solved with a second order accurate numerical scheme [10]. Convergence was considered achieved when mass and turbulence residuals were below 10^{-4} and energy residual was below 10^{-7}.

5. Results and discussion

The 30 consecutive cycles analyzed were characterized by 12 hours at most of charging followed by 12 hours of discharging with an air mass flow rate, through each TES unit, of 89.6 kg/sec for both the phases. However, especially for the first cycles, a discharge phase of 12 hours would have led to a too low HTF outlet temperature. Because of that, besides the temporal constraint, the discharge phase was considered completed once the HTF outlet temperature from the TES was equal to 600 °C. With this further constraint, the only discharge phase with a duration sensibly lower than 12 hours was the first one lasting for about 10 hours. The second discharge showed a duration of about 11 hours and 30 minutes and, from the fifth discharge phase on, the TES was able to provide an HTF outlet temperature higher than 600 °C for the 12 hours.

The CFD simulations results are presented in terms of temperature distribution, of the TES system, at different time spans. Non-dimensional quantities were exploited to describe the results obtained; non-dimensional position and temperature of unity indicate the upper surface, and the highest temperature respectively, of the packed bed. Non-dimensional position is obtained by dividing the dimensional axial position with respect to the total packed bed height; while, non-dimensional temperature is given by the ratio of the resulting temperature, of the layer under investigation, minus the minimum temperature of the packed bed, at the instant of time considered, divided by the difference between the maximum and the minimum temperature of the packed bed at the same instant of time. Figure 2 shows the result obtained in terms of temperature distribution into the packed bed as a function of the axial position. Left-hand side of Fig. 2 focuses on the temperature distribution at the end of some of all the charge phases analyzed; conversely, in the r.h.s. of Fig. 2, the end of the corresponding discharge phases is reported. An important

consideration that can be drawn is that, during the initial cycles, the TES undergoes a sharp variation of thermal stratification. This is due to the fact that, at the beginning of the CFD simulation the TES system was assumed to be in its dead-state; the effect of having both the charging and discharging temperatures different from that of the initialization led to the creation of two separate thermocline zones into the packed bed. This phenomenon was already observed in a previous study [9] in which 15 consecutive cycles only where analyzed. The additional cycles simulated here allowed to confirm that the double thermocline effect disappears towards the end of the 30 cycles analyzed. From a graphical standpoint, Fig. 3 shows the temperature contours of the TES system at the end of several consecutive charge phases.

The result obtained in terms of transient evolution of thermal stratification is reported in Fig. 4. The markers represent the average value of the stratification efficiency of all the phases analyzed. To obtain these average values, six instantaneous stratification efficiency indexes were computed for each phase corresponding to an interval of about two simulation hours between one instant of time and the following.

The highest value of stratification efficiency, of about 0.93 on average, was achieved during the first charge indicating that the thermal stratification of the TES system is comparable to the ideal case of perfectly stratified TES. The stratification efficiency sensibly decreases down to 0.58, on average, already for the consecutive discharge phase indicating an entropy generation increment given by the creation of the two thermocline zones into the packed bed. A minimum value of stratification efficiency can be observed, for both the charge and discharge phases, between the 5th– 6th cycle.

The difference between the average stratification efficiency of the charge and discharge phases reduces with consecutive cycles disappearing towards the 19th– 20th cycle wherein a maximum is also achieved and the two thermocline zones merge with each other into a single one. From this point forward, the stratification efficiency slightly decreases until reaching a stable condition of about 0.65.

An important consideration that can be drawn, looking at the result obtained with the aforementioned assumptions and approximations, is that about 28-30 cycles are required by the system before achieving a stable thermal stratification into the packed bed. Considering that a single cycle corresponds to one day, the transient behavior of the TES system is in the order of one month. Pre-charging the TES system, i.e. charging completely the storage at the temperature equal to the lower reference temperature of the system, before the first cycle might be a valuable solution to sensibly reduce the long time required to achieve a stable condition.

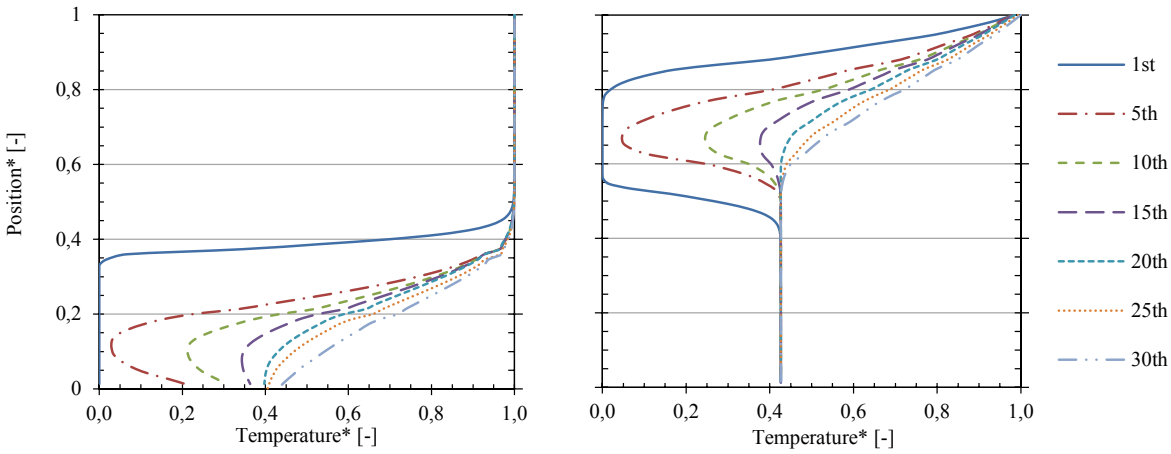

Fig. 2: Non-dimensional temperature as a function of packed bed height at the end of some charge (l.h.s.) and discharging (r.h.s.) phases.

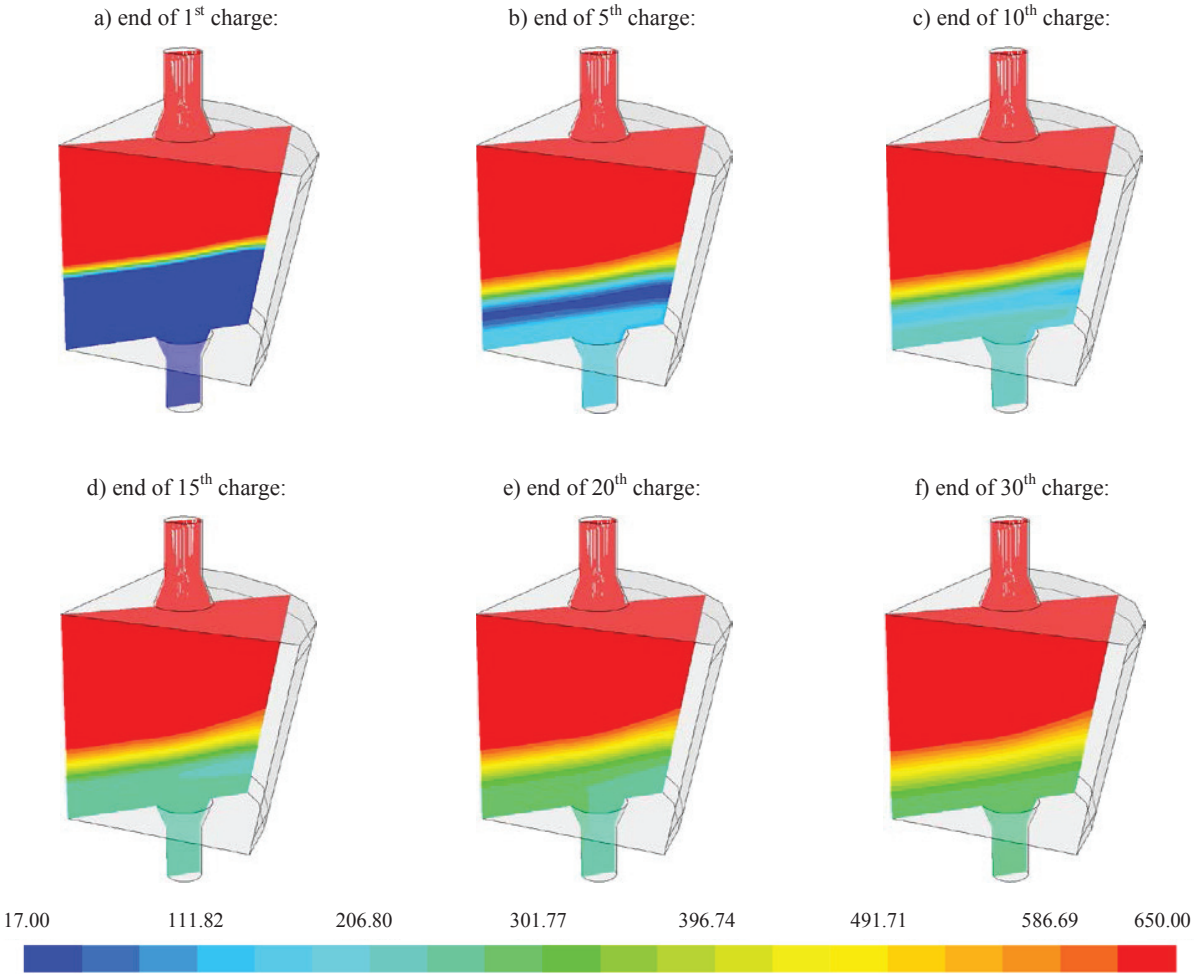

Fig. 3: Temperature contours of the TES system at the end of several consecutive charge phases. Temperature values are [°C].

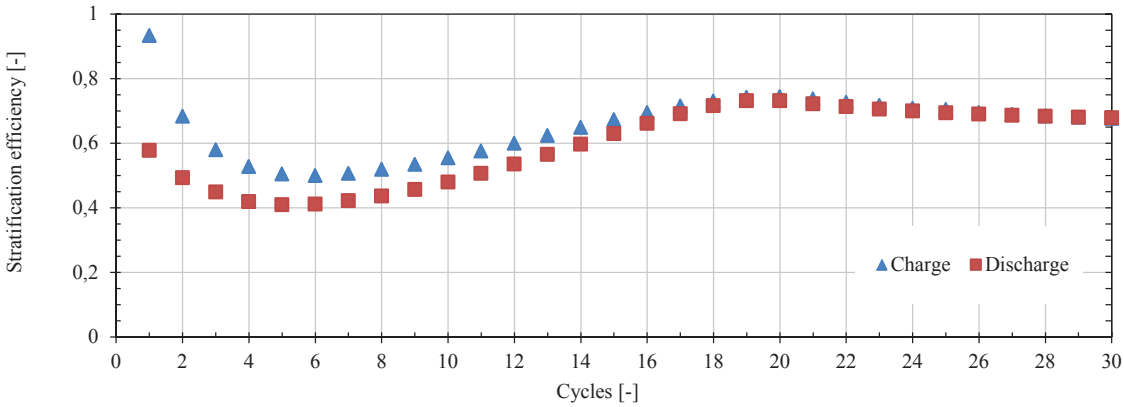

Fig. 4: Average transient stratification efficiency for consecutive charge/discharge cycles.

6. Conclusions

The thermo-fluid dynamics behavior of a single-tank TES system, with gravel as low-cost filler material, was obtained by means of accurate time-dependent 3D CFD simulations. The system was analyzed, under 30 consecutive cycles of charge and discharge phases in order to evaluate the effect of the initial cycles on the thermal stratification. The latter, qualitatively evaluated with a second-law based figure of merit, showed a strong variation lasting for 20-22 cycles. A stable thermal stratification into the packed bed was achieved towards the end of the 30 cycles analyzed. The long transient behavior is the result of the two thermocline zones, observed into the packed bed for the first 19-20 cycles, given by the start up of the TES. Pre-charging the TES system before the first cycle might be a valuable solution to sensibly reduce the long time required to achieve a stable thermal stratification.

Acknowledgements

This work has been developed in the framework of the SolAir-3 Project ("SI/500926") financed by the Swiss Federal Office of Energy (SFOE - OFEN - BFE). Furthermore, the support to the development of this work by the Swiss Center of Competence in Energy Research framework (SCCER 3 - Energy Storage) is kindly acknowledged.

References

[1] Libby C., "Solar Thermocline Storage Systems - Preliminary design study", Electric Power Research Institute (EPRI), 2010.
[2] Pedretti A., "A 3 MW thermal CSP pilot plant in Morocco with the Airlight Energy technology", SolarPACES Conference, 2012.
[3] Dinçer I., Rosen M., "Thermal Energy Storage: Systems and Applications - Second Edition", United Kingdom: John Wiley & Sons, 2011.
[4] Haller M., Cruickshank C., Streicher W., Harrison S., Andersen E., Furbo S., "Methods to determine stratification efficiency of thermal energy storage processes – Review and theoretical comparison", Solar Energy, vol. 83, pp. 1847 – 1860, 2009.
[5] Panthalookaran V., Heidemann W., Müller-Steinhagen H., "A new method of characterization for stratified thermal energy stores", Solar Energy, vol. 81, no. 8, pp. 1043 – 1054, 2007.
[6] Njoku H., Ekechukwu O., Onyegegbu S., "Analysis of stratified thermal storage systems: An overview", Heat & Mass Transfer 50, 2014.
[7] Çengel Y., Boles M., "Thermodynamics: An engineering approach – 5th edition", 2006.
[8] Good P., Zanganeh G., Ambrosetti G., Barbato M.C., Pedretti A., Steinfeld A., "Towards a commercial parabolic trough CSP system using air as heat transfer fluid", Energy Procedia, vol. 49, pp. 381–385, 2014.
[9] Zavattoni S.A., Barbato M.C., Pedretti A., Zanganeh G., Steinfeld A., "High temperature rock-bed TES system suitable for industrial-scale CSP plant – CFD analysis under charge/discharge cyclic conditions", Energy Procedia, vol. 46, pp. 124 - 133, 2014.
[10] Versteeg H., Malalasekera W., "An introduction to computational fluid dynamics: the finite volume method approach", Longman 1995.
[11] Shih W., Liou, A., Shabbir Z., Yang and J. Zhu, "A new k-epsilon eddy-viscosity model for high Reynolds number turbulent flows - Model development and validation", Computers and Fluids, vol. 24, no. 3, pp. 227-283, 1995.
[12] Launder B., Spalding D., "The numerical computation of turbulent flows", App. Mech. & Eng. 3, no. 2, pp. 269 - 289, 1974.
[13] ANSYS, FLUENT - Theory guide, 2012.
[14] ANSYS, FLUENT - User's guide, 2012.
[15] Vafai K., "Handbook of Porous Media", New York: Marcel Dekker, Inc., 2000.
[16] Nield D.A., Bejan A., "Convection in porous media - Third edition", USA: Springer, 2006.
[17] Kaviany M. "Principle of heat transfer in porous media, 2nd edition", Springer, 1995.
[18] Yagi S., Kunii D., "Studies on effective thermal conductivities in packed beds", A.I.Ch.E. Journal, vol. 3, no. 3, pp. 373-381, 1957.
[19] Kunii D., Smith J.M., "Heat transfer characteristics of porous rocks", A.I.Ch.E. Journal, vol 6, no. 1, pp. 71-78, 1960.
[20] Zavattoni S., Barbato M., Pedretti A., Zanganeh G., Steinfeld A., "Effective thermal conductivity and axial porosity distribution of a rock-bed TES system: CFD modeling and experimental validation", SolarPACES Conference, September 11–14, Marrakech, Morocco, 2012.
[21] Scheidegger A.E., "The physics of fluid flow through porous media. Third edition", Toronto: University of Toronto Press, 1974.
[22] Martin H. "Low Peclet number particle-to-fluid heat and mass transfer in packed beds." Chem. Eng. Science 33, no. 7, pp. 913-919, 1978.
[23] Zavattoni, S.A., Barbato M.C., Pedretti A., Zanganeh G., "CFD simulations of a pebble-bed Thermal Energy Storage system accounting for porosity variations effects", 17th SolarPACES Conference, Paper ID: 24636, September 20–23, Granada, Spain, 2011.
[24] Zanganeh G., Pedretti A., Zavattoni S., Barbato M., Steinfeld A., "Packed-bed thermal storage for concentrated solar power - Pilot-scale demonstration and industrial-scale design", Solar Energy, vol. 86, pp. 3084 - 3098, 2012.
[25] De Klerk A., "Voidage variation in packed beds at small column to particle diameter ratio", A.I.Ch.E. J. 49, no. 8, pp. 2022 - 2029, 2003.
[26] Ergun S., "Fluid flow through packed columns", Chemical Engineering Progress, vol. 48, pp. 89-94, 1952.
[27] Incropera F.P., Dewitt D., Bergman T, Lavine A., "Fundamentals of heat and mass transfer, 6th edition", John Wiley & Sons, 2007.
[28] Somerton, W.H., "Thermal properties and temperature-related behavior of rock/fluid systems", Elsevier, New York NY, 1992.
[30] Kelley, K., "Contribution to the data on theoretical metallurgy XIII. High-temperature heatcontent, heat-capacity, and entropy data for the elements and inorganic compounds", 1960.